EXPECTED LEVEL OF SELF-COMPTON SCATTERING IN RADIO LOUD QUASARS

Steven D. Bloom and Alan P. Marscher

Department of Astronomy, Boston University

Abstract

Radio-loud quasars usually contain parsec-scale nonthermal jets. The most compact emission region ("the core"), and perhaps some of the moving "knots," are expected to be efficient producers of inverse Compton scattered X-rays and γ-rays since many of the synchrotron photons will upscatter before escaping. Through multifrequency flux density observations and VLBI measurements of angular sizes, one can predict the flux density of this self-Compton high-energy emission. It is not always the case that the brightest synchrotron sources are also the brightest X-ray and γ-ray sources. Perhaps a better predictor of high-energy brightness is the ratio of hard X-ray to high-frequency radio emission.

Using the synchrotron self-Compton relations, we predict the γ-ray fluxes of several sources we expect to be detected by EGRET. More accurate predictions will be made when we complete a program of contemporaneous radio-submillimeter and X-ray observations during the course of the EGRET all-sky survey.

1. INTRODUCTION

VLBI observations of the parsec-scale structure of quasars show that the radio jets are extremely luminous, suggesting high energy densities of soft photons. It is expected that the synchrotron photons will scatter off the relativistic electrons that produced them to create X-rays and possibly soft γ-rays. Second order scattering should produce hard γ-rays. The synchrotron self-Compton (SSC) process has been discussed in the context of quasars by several authors (e.g., Jones, O'Dell and Stein , 1974; Ghisselini, Maraschi, and Treves, 1985; Band and Grindlay, 1986; Marscher 1987). The large X-ray data base provided by the *Einstein Observatory* has made it feasible to test the relationship between radio and high-energy emission, at least in a statistical sense. Several authors show that a strong correlation exists between X-ray and radio emission (Owen, Helfand, and Spangler 1981; Worrall *et al.* 1987; Kembhavi, Feigelson, and Singh 1986; Browne and Murphy 1987). Also, 3C273 and 3C279, both strong radio sources, have been detected in γ-rays . These results would suggest a one-to-one correspondence between the high-energy flux and radio flux. However, a more detailed look at self-Compton theory shows that the X-ray flux density $F_{\nu x}$ will have, in addition to a dependence on the radio flux density, a strong dependence on several other parameters (e.g., angular size). Similar calculations can be extended to the second order Compton flux densities. The dependence on several parameters is even more extreme in this case. Modest uncertainties in these parameters are typical; thus, predictions for the γ-ray flux density made in this manner are quite rough. There is then sufficient reason to seek an alternative method of predicting the γ-ray flux density. We show that if

the X-ray flux density is measured, then the *ratio* $F_{\nu x}/F_{\nu r}$ can be used to predict $F_{\nu\gamma}/F_{\nu x}$. This method was discussed by Jones (1979); we present more precise formulae. Flux densities at energies within the EGRET band can then be predicted.

2. FIRST AND SECOND ORDER SCATTERING RELATIONSHIPS

For homogeneous sources with simple geometries (e.g., a sphere), the predicted X-ray flux density can be calculated using the standard expressions for first order scattering emissivities in the Thomson limit (Blumenthal and Gould 1970; Gould 1979; Rybicki and Lightman 1979; Hughes and Miller 1991). The first order flux density then has the following dependence on the physical parameters of the source:

$$F_\nu{}^{1C} \propto N_0 R F_\nu{}^S ln(\nu_u/\nu_m) \propto N_0{}^2 B^{\frac{(1+p)}{2}} R^4 D^{-2} ln(\nu_u/\nu_m). \quad (1)$$

Here, R is the radius of the source, and D is the distance. Using expressions for the synchrotron flux density and optical depth at spectral turnover for a self-absorbed synchrotron source, one can solve for B, the magnetic field stength, and the parameter N_0, where the number density of relativistic electrons of a given energy follows the relationship $N(E) \propto N_0 E^{-p}$, in terms of *observable* radio source properties. These expressions for the physical parameters are then substituted back into the derived equation for X-ray flux density (see Marscher 1987 for details). The major result is that the first order flux density at photon energy E_{keV} keV is highly dependent on these parameters:

$$F_\nu{}^{1C} \propto \theta^{-2(p+2)} F_m{}^{p+3} \nu_m{}^{-(3p+7)/2} E_{keV}{}^{(1-p)/2} ln(\nu_u/\nu_m) \left(\frac{1+z}{\delta}\right)^{p+3}. \quad (2)$$

Here, F_m and ν_m are the flux density and frequency at spectral turnover, z is the redshift, δ is the Doppler beaming factor (a correction for bulk relativistic motion within the source), and the optically thin $\log F_\nu{}^S$ vs. $\log \nu$ spectrum is assumed to be a power law of slope $(1-p)/2$ between frequencies ν_m and ν_u. In the remaining proportionalities, we will ignore the slowly varying logarithmic term.

The second order flux density is then even more strongly dependent on the observable parameters (due to an extra factor of $N_0 R$):

$$F_\nu{}^{2C} \propto N_0 R F_\nu{}^{1C} \propto (N_0 R)^2 F_\nu{}^S \propto \theta^{-4(p+2)} \nu_m{}^{-(7p+13)/2} F_m{}^{2p+5} \left(\frac{1+z}{\delta}\right)^{2(p+3)}. \quad (3)$$

Usually, real sources cannot be well modeled as a single homogeneous sphere; however, the VLBI components collectively can be approximated as a composite of homogeneous spheres (Marscher 1987). The predicted flux densities for each component are then added together and compared to the measured flux density. Such calculations are usually assumed to be in the Thomson limit ($h\nu_{initial} << mc^2/\gamma$) or in the extreme Klein-Nishina limit ($h\nu_{initial} \gtrsim mc^2/\gamma$) because the full expression for the electron differential cross section that goes into calculating the emissivities is greatly simplified in these two limits. However, to

a first approximation, the basic proportionalities of the first and second order flux densities on these radio source parameters are independent of these assumptions. More precise expressions, which explicitly use the full Klein-Nishina cross section, are discussed below.

Ideally, we would like to obtain an expression for predicting the γ-ray flux density that is not so highly dependent on parameters that are poorly known. We can see from expressions (1) and (3) that the ratio of second order (γ-ray) to first order (X-ray) self-Compton flux densities equals the ratio of the first order self-Compton to synchrotron flux density. Therefore, if the ratio $F_{\nu x}/F_{\nu r}$ is *measured* and assumed to be determined by the SSC process, $F_{\nu\gamma}/F_{\nu x}$ can be predicted without knowledge of the radio source parameters. For the first order Compton emissivity, it is safe to assume that the Thomson limit applies. However, for the second order emissivity the Thomson limit will only apply over a fraction of the spectrum. Thus we need to integrate numerically the full expression of Blumenthal and Gould (their eq. 2.75). Performing this calculation, we obtain:

$$F_\nu{}^{2C} = 3^{\frac{(3-p)}{2}} 2^{2p-3} \sigma_T{}^2 (mc^2)^{2(1-p)} F_1(p) N_0^2 R^2 F_\nu{}^S S(\frac{\nu_S}{\nu_2})^{\frac{p-1}{2}} \ln(\frac{\nu_u}{\nu_m}). \quad (4)$$

Here, ν_1 is the first order photon frequency, ν_2 is the second order photon frequency, and $F_1(p)$ is that of Hughes and Miller (1991). The parameter S represents the integral:

$$S(\nu_1, \nu_2, q) = \frac{\int d\nu_1 I_\nu(\nu_1) \nu_1{}^{\frac{(p-3)}{2}} \int_0{}^1 dq\, f(q, \nu_1, \nu_2)}{K_{1C}}. \quad (5)$$

Here, $I_\nu(\nu_1)$ is the first order self-Compton intensity, $K_{1C} \equiv I_\nu(\nu_1)\nu_1{}^{\frac{(p-1)}{2}}$ is the first order intensity without the frequency dependence, f is the complicated function in equation (2.75) of Blumenthal and Gould, and $q \equiv \frac{\nu_2}{4\gamma\nu_1(1-h\nu_1/mc^2)}$. The integral S is only weakly dependent on the upper and lower limits of the first order Compton spectrum and spectral index, and is of order unity. We can now solve for $F_{\nu\gamma}/F_{\nu x}$ in terms of $F_{\nu x}/F_{\nu r}$:

$$\frac{F_{\nu\gamma}}{F_{\nu x}} = \frac{3^{\frac{(p+1)}{2}}}{2} \left(\frac{F_{\nu x}}{F_{\nu r}}\right) \frac{S(\nu_2, \nu_1, q)}{F_1(p) ln(\nu_u/\nu_m)} \left(\frac{\nu_2 \nu_r}{\nu_1{}^2}\right)^{\frac{(1-p)}{2}}. \quad (6)$$

We must emphasize that using this equation does not eliminate all of the uncertainty of expression (3). For instance, a rigorous analysis would require calculating this ratio for each separate component of the radio source, which is not possible due to the comparatively low resolution of current X-ray and γ-ray instrumentation. Possible source variability in either the radio or X-rays will lead to inaccurate estimates of $F_{\nu x}/F_{\nu r}$ unless the measurements are nearly simultaneous. In addition, the Thomson limit is not valid over much of the γ-ray range. In this case, numerical calculations are required (see Marscher and Bloom, these proceedings).

We present the results of a numerical computation of the self-Compton spectrum of a model uniform source in Figure 1. Note that there is substantial curvature to the spectrum of the self-Compton emission, contrary to the popular myth that it is a power law over most X-ray and γ-ray energies.

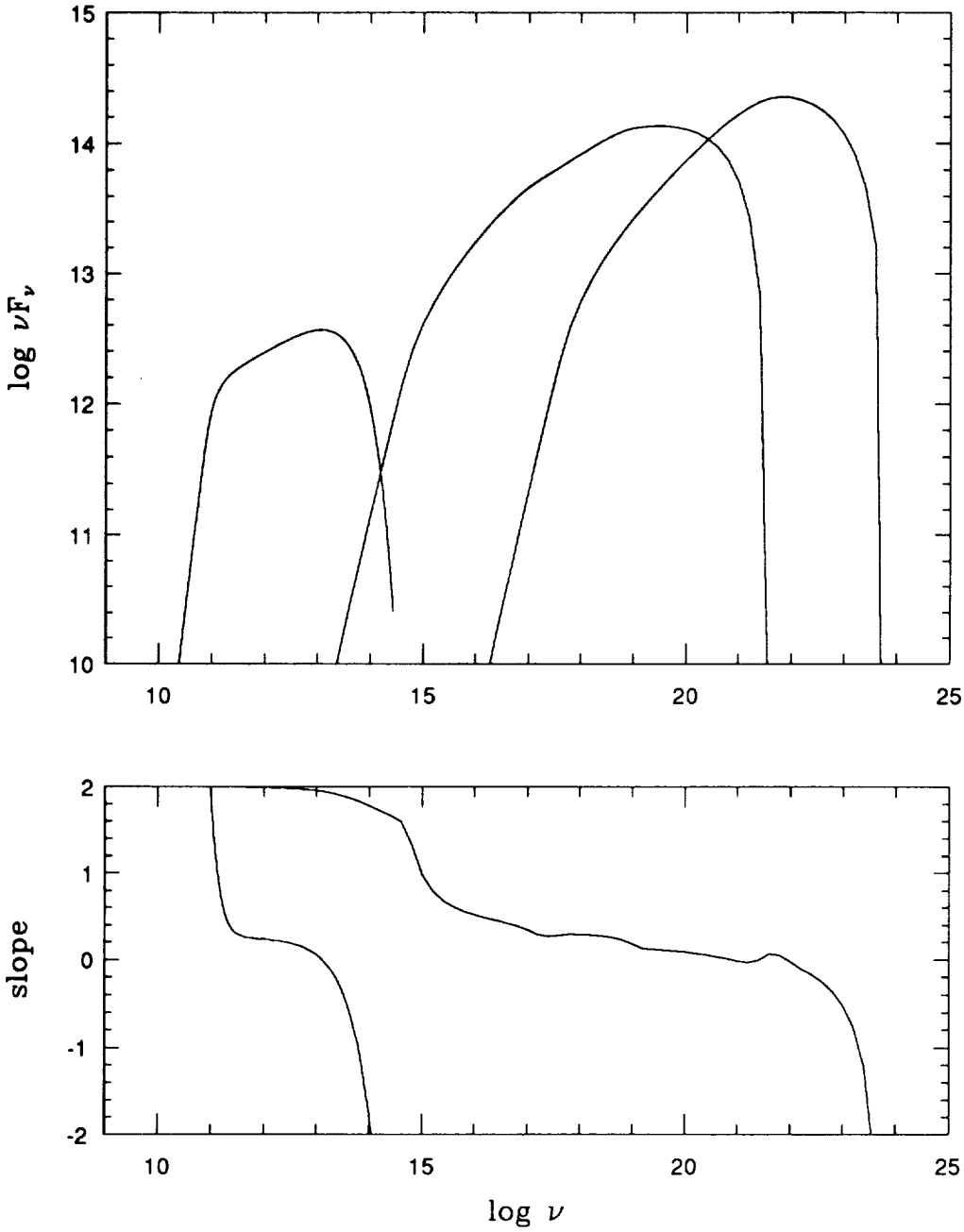

Figure 1 νF_ν spectrum of the synchrotron (left-most curve), first order self-Compton (middle curve), and second order self-Compton (right-most curve) emission from a model spherical, uniform, nonthermal source. The lower panel gives the slope of the νF_ν synchrotron (left-hand) and first + second order self-Compton (right-hand) spectrum as a function of frequency.

Equation (6) is still practical, especially if the detailed observations required for analysis of expression (3) are uncertain or non-existent. The best procedure would be to use both methods whenever the observations allow.

3. PREDICTIONS

Using equation (6) and taking the accompanying caveats to heart, we can predict which sources are likely to be detected by EGRET. We would like to find a sample of sources with recent simultaneous radio core and X-ray flux density measurements. Such a sample does not yet exist; however, Bloom and Marscher (1991) have compiled the X-ray data for all quasars and active galactic nuclei observed with both *Einstein Observatory* and with VLBI. We use these data as a rough guideline to predict $F_{\nu\gamma}$, although these calcuations are only valid for the epoch of the X-ray and radio observations, 1979-1981. Table 1 shows sources with highest values of predicted γ-ray flux that are above 5×10^{-8} photons cm^{-2} s^{-1}, the flux limit of EGRET (Kanbach 1989). The second column gives the X-ray flux density at 2 keV as measured by *Einstein*; the third column gives the measured ratio of X-ray flux density at 2 keV to the core radio flux density at 10.7 GHz in 1980; the fourth column gives the predicted ratio of γ-ray flux density at 100 MeV to X-ray flux density; and the last column gives the predicted photon flux in the EGRET band, integrated numerically between 100 MeV and 30 GeV . We have included effects due to the Klein-Nishina electron cross-section, which is significant at this energy range. We notice that some of the sources with high predicted γ-ray fluxes have rather modest X-ray and radio flux densities, implying again that it is not sufficient to use radio or X-ray flux alone as an indicator of which sources will be brightest in γ-rays. We see from equation (4) that the main requirement is that the source be compact. Alternatively, from expressions (1) and (3) we see that the γ-ray flux is proportional to ${N_0}^3$ and is therefore strongly dependent on the relativistic electron density within the source.

Table 1. Predicted γ-ray Fluxes, Epoch 1980

Source	$F_{\nu x}$ (μJy)	$\frac{F_{\nu x}}{F_{\nu r}}$ (10^{-6})	$\frac{F_{\nu\gamma}}{F_{\nu x}}$ (10^{-4})	F_γ (10^{-7}phot cm^{-2} s^{-1})
NRAO 140	1.65	2.8	3.6	0.9
3C 111	1.87	1.7	2.2	0.6
3C 120	5.2	5.8	7.7	6.0
3C 249.1	0.47	13.4	17.7	1.3
ON 231	0.31	0.4	0.5	0.02
3C 273	7.9	0.8	1.04	1.3
3C 279	0.40	0.1	0.1	0.01
3C 334	0.15	2.8	3.7	0.08
Mkn 501	7.4	11.2	14.8	17
1721+343	1.4	14.0	18.5	3.1
3C 390.3	1.0	2.4	3.2	0.5
BL Lac	1.87	1.9	2.5	0.7
3C 446	0.48	0.2	0.3	0.02

We note that the predicted γ-ray fluxes of several of the sources in Table 1 (especially Mkn 501) were above the detection level of COS-B. This result would imply that some of these sources (such as the BL Lac objects) are probably creating X-rays through some process other than the SSC mechanism. The predicted flux for 3C273, on the other hand, is approximately the same as that measured by COS-B (Swanenburg *et al.* 1978; see also Jones 1979). The predicted flux for 3C 279 is well below that recently measured by EGRET. This low prediction, which is based on X-ray and radio flux densities from 1980, is consistent with the non-detection of 3C 279 by COS-B. In addition, the radio flux at centimeter and millimeter wavelengths was considerably lower at the time of COS-B observations. For instance, the total flux density at 90 GHz went from 7-8 Jy in 1976-1978 (Landau *et al.* 1980) to approximately 14 Jy in July 1991 (extrapolated from the 150 GHz flux density; Robson 1991).

During 1991, 3C 279 has been flaring at millimeter and infrared wavelengths (Robson 1991). The self-Compton process acts as an amplifier of the synchrotron flare, leading to a very high γ-ray flux, as observed. Other quasars currently undergoing synchrotron flares are the bright radio quasar 4C 39.25 and the high $F_{\nu x}/F_{\nu r}$ quasar NRAO 140. We predict that these sources will also be detected by EGRET.

4. CONCLUSIONS

Compton theory for homogeneous sources shows that the second order flux density can be predicted if the ratio $F_{\nu x}/F_{\nu r}$ is measured. Equation (6) can then be used to estimate the γ-ray flux. However, it is clear from the predictions in section 4 that a more accurate analysis, looking at each component of the radio source and applying the first and second order scattering relationships, is necessary to test the dominance of the SSC process. Future work that will include multiwavelength VLBI radio and submillimeter radio observations at times close to ROSAT observations will allow for more reliable measurements of $F_{\nu x}/F_{\nu r}$, and a detailed component-by-component analysis for a number of quasars. Accurate fluxes can then be predicted and compared with EGRET observations.

REFERENCES

Band, D. L. , and Grindlay, J. E. 1986, *Ap. J.*, **308**, 576.

Bloom, S. D. , and Marscher, A. P. 1991, *Ap. J.*,**366**,16.

Blumenthal, G. R. and Gould, R. J. 1970, *Rev. Mod. Phys.*, **42**, 1970.

Browne, I. W. A., and Murphy, D. W. 1987, *M.N.R.A.S.*, **226**, 601.

Ghisselini, G. , Maraschi, L. , and Treves, A. 1985 , *Astr. Ap.*, **146**, 204.

Gould, R. J. 1979, *Astr. Ap.*, **76**, 306.

Hughes, P. A. , and Miller L. 1991, in *Beams and Jets in Astrophysics*, ed. P. A. Hughes (Cambridge: Cambridge University Press), p. 1.

Jones, T. W. 1979, *Ap. J.*, **233**, 796.

Jones, T. W. , O'Dell, S .L. , Stein, W. A. 1974, *Ap. J.*, **188**, 353.

Kanbach, G. *et al.* 1989 in *Proceedings of the Gamma Ray Observatory Workshop*, ed. W. N. Johnson (NASA: Washington, D.C.), p. 2-7.

Kembhavi, A. , Feigelson, E. D. , and Singh, K. P. 1986, *M.N.R.A.S.*, **220**, 51.

Landau, R. *et al.* 1980, *A.J.*, **85**, 363.

Marscher, A. P. 1987, in *Superluminal Radio Sources*, ed. J. A. Zensus, and T. J. Pearson (Cambridge: Cambridge University Press), p. 280.

Owen, F. N., Helfand, D. J., and Spangler, S. R. 1981, *Ap. J. (Letters)*, **250**, L55.

Robson, E. I. 1991, private communication.

Rybicki, G. B. , and Lightman, A. P. 1979, *Radiative Processes in Astrophysics* (New York: Wiley).

Swanenburg, B. N., *et al.* 1978, *Nature*, **275**, 298.

Worrall, D. M. , Giommi, P. , Tananbaum, H. , and Zamorani, G. 1987, *Ap. J.*, **313**, 596.